J. Condensed Matter Nucl. Sci. 37 (2023) 9–22

Research Article

Transmutation of Palladium Induced by Laser Irradiation

Jean-Paul Biberian

Aix-Marseille Université, France

Lawrence Forsley and Pamela Mosier-Boss

Global Energy Corporation, USA.

Abstract

Ubaldo Mastromatteo published in 2016, a very simple experiment where he directed a laser beam on a thin film of palladium deposited on a silicon oxide substrate in H_2 and D_2 atmospheres. By SEM he showed formation of many new elements. In this study, we made a similar experiment with identical samples in H_2 and D_2. Both experiments lasted 3 months. The laser used was a 5 mW 650 nm red pointer laser. What surprised us is that in a particular 180 µm diameter spot, many new elements appeared that were not there before, and in some parts of the spot the palladium had totally disappeared. The experiments were analyzed by SEM and neutrons were potentially observed with CR-39.

Keywords:

1. Introduction

Since the announcement of the discovery of cold fusion by Martin Fleischmann and Stanley Pons in March 1989, many different techniques have been employed to reproduce their initial work and to try to find new effects. Transmutation has always been a candidate of choice, since if nuclear reactions occur, some nuclear effect should be measured either by radiation or by formation of new elements. In heavy water electrolysis experiments with palladium cathodes, it has been shown by several authors the presence of helium-4 [1,2]. This can be understood as a fusion of two deuterium atoms. However, several authors have also shown that other elements can be found. In a palladium cathode that produced a lot of anomalous heat it has been shown that one isotope of silver was present at the surface of the palladium cathode [3]. Many other experiments have shown transmutation of the main element [4]. All the results detailed above were produced during a reaction where there was activation, though several authors have also demonstrated that simply in the presence of hydrogen or deuterium some transmutations could occur. Mastromatteo [5] performed an experiment where he used a laser beam as activation and shined it onto a palladium film deposited on a silicon substrate in hydrogen and deuterium atmospheres. After two weeks of irradiation, he analyzed the surface with scanning electron microscopy and found many new elements, not present before. Mastromatteo gave to one of us (Jean-Paul Biberian) two identical samples to reproduce his work.

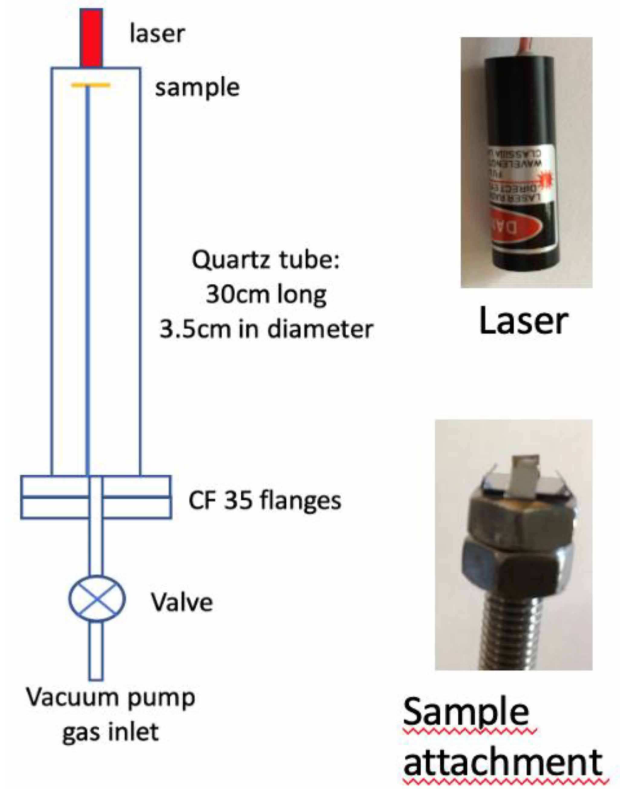

Figure 1. Experimental set-up

2. Experimental Set-Up

The sample has the following structure: a silicon wafer with a thermal oxide layer (about 500 nm), then a thin layer of titanium (30 nm) for adhesion of the palladium film (500 nm). Figure 1 shows a schematic of the vacuum chamber with the laser on top aimed at the silicon chip covered with a palladium film. The 5 mW, 650 nm red laser (no brand name) is not focused, therefore it covers an area of about 4 mm^2. The chamber is a 30 cm long 30 mm in diameter quartz tube. It is evacuated with a mechanical pump down to about $2x10^{-2}$ mBar, then hydrogen gas is introduced at a pressure of about 2 bars (absolute pressure). The sample is placed on top of an 8 mm stainless steel rod and attached to it with four stainless steel foils as shown in Figure 1. Experiments have been performed with hydrogen and deuterium with two identical samples. Each one being 1 cm^2 silicon chip with a 250 nm thin film of palladium deposited at their surfaces. Both experiments lasted about three months.

3. SEM-EDX Analysis of the Sample Under Hydrogen

At the end of the experiments the samples were analyzed by Scanning Electron Microscopy (Jeol JSM-6340F) and EDX (BRUKER Esprit) for elemental chemical analysis. Several spots have been identified with anomalous composi-

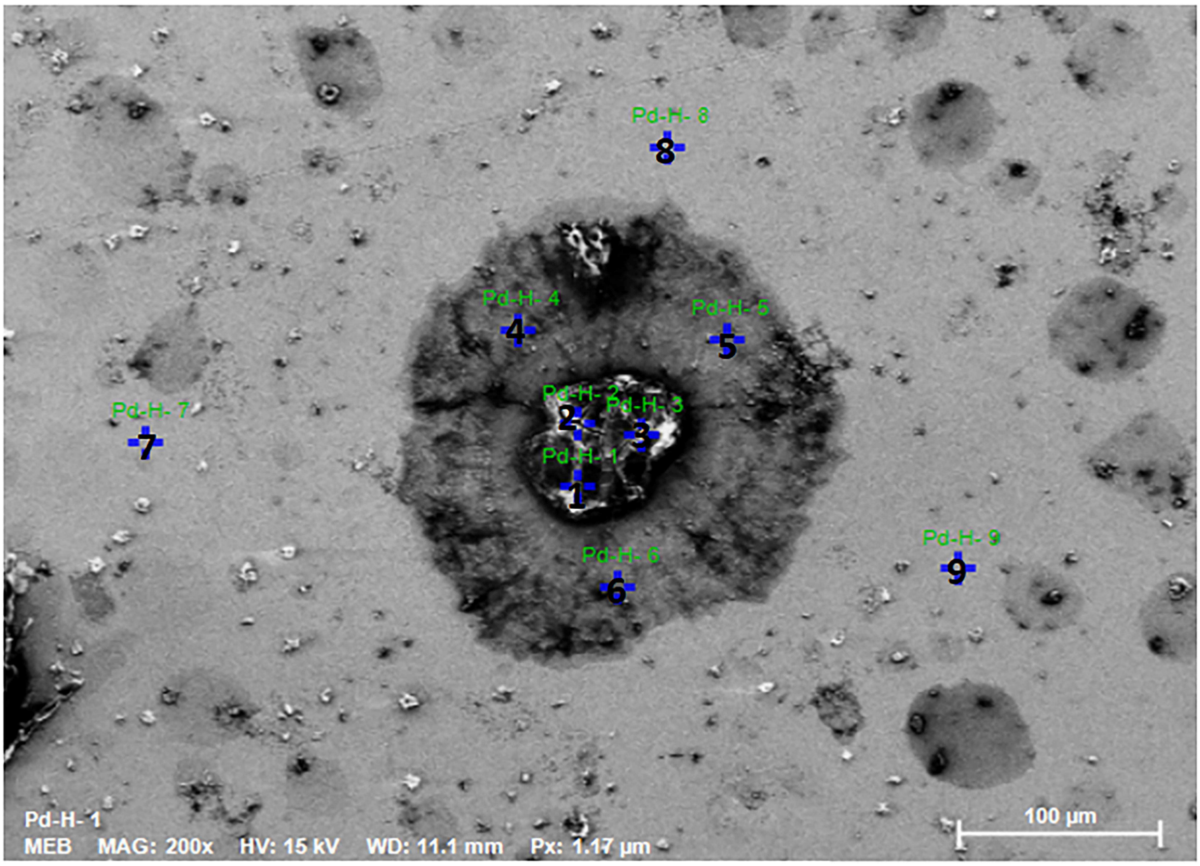

Figure 2. SEM image showing a large hot spot and several smaller ones. Elemental analysis has been made in three different areas of the hot spot and outside of the spot.

tion, but the largest one was located at the center of the sample. Figure 2 shows a picture of this largest spot of about 180 µm in diameter. Several smaller hot spots are also visible on this photo. We have performed EDX analysis of the chemical composition of the anomalous spot: 3 analysis points at the center in the dark area, 3 in the grey area, and 3 outside of the hot spot in a light area. Concentrations are given in atomic percentages. The new elements do not appear uniformly under the laser beam irradiation, it is very possible that nuclear reactions occur only at specific places, maybe crystal defects, like dislocations, grain boundaries or cracks.

3.1. Central Area

Points 1-2 and 3 indicated in Figure 2 have been analyzed:

Point 1

N: 10.44%, O: 68.22%, Na: 6.44%, Al: 0.42%, Si: 0.24%, P: 0.07%, S: 1.46%, Mn: 0.14%, Fe: 2.94%, Ni: 8.83%, Zn:0.53%, Pd: 0.25%

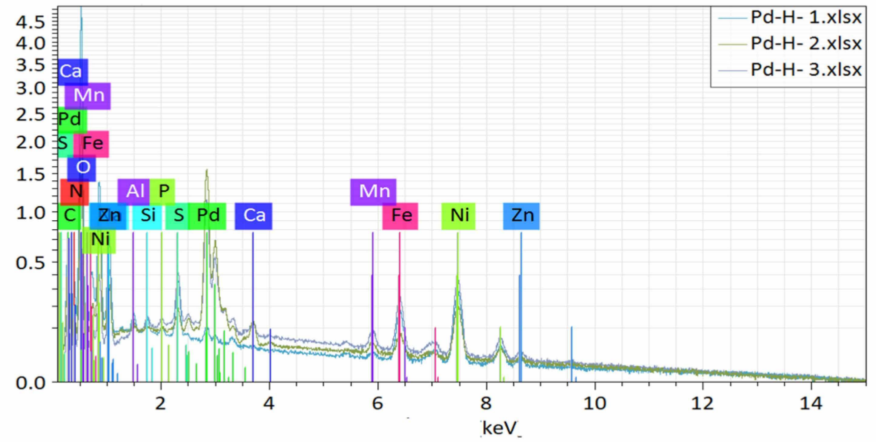

Figure 3. EDX spectra of the three points analyzed in the central area.

Point 2

N: 14.55%, O: 67.06%, Na: 2.17%, Ca: 0.68%, Mn: 0.42%, Fe: 1.05%, Ni: 6.08%, Zn: 0.40%, Mo: 0.29%, Pd: 7.28%

Point 3

N: 11.09%, 0: 52.11%, Na: 5.60%, S: 2.12%, Ca: 0.46%, Mn: 1.13%, Fe: 5.34%, Ni: 15.08%, Pd: 7.04%

The central area analysis shows that almost all the palladium has disappeared. Some elements like Nitrogen, Oxygen, Sodium, Sulfur, Manganese, Iron and Nickel are easily detected. The elements Calcium, Aluminum, Zinc and Molybdenum are below the 1% concentration detection limit, but they are however still visible on the spectra. It is surprising to see large quantities of nitrogen and oxygen. See Figure 3 for details.

3.2. Grey Area

Points 4- 5 and 6 indicated in Figure 2 have been analyzed:

Point 4

N: 18.59%, O: 58.75%, Na: 1.58%, Fe: 0.70%, Ni: 2.98%, Pd: 17.40%

Point 5

O: 41.68%, Na: 2.87, Pd: 55.45%

Point 6

N: 13.88%, O: 56.39%, Na: 2.00%, Fe: 0.75%, Ni: 1.57%, Pd: 25.41%

The reaction is less efficient than at the central points, with fewer elements. Some elements are below the 1% limit. However, there are elements measured with certainty: Nitrogen, Oxygen, Sodium, Nickel. Iron is also present, but at low level. See Figure 4 for details.

3.3. Light Area

Points 7-8 and 9 indicated in Figure 2 have been analyzed

Point 7

O: 4.40%, Pd: 95.60%

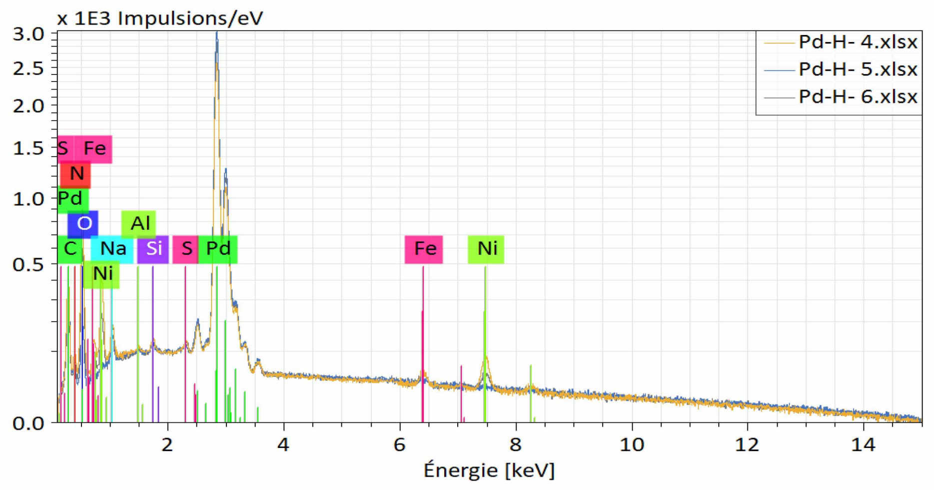

Figure 4. EDX spectra of the three points analyzed in the grey area.

Point 8
O: 3.58%, Pd: 96.42%
Point 9
O: 5.84%, Pd: 94.16%
Almost only palladium and a few percent of oxygen, probably due to contamination. See Figure 5 for details.

4. SEM-EDX Analysis of the Sample Under Deuterium

The experiment with the second sample in deuterium atmosphere was performed under same conditions as for hydrogen. However, contrary to the hydrogen sample, no hot spot was observed. Figure 6 shows as SEM image of the sample surface.

As shown in Figure 7, there is almost only palladium present at the surface:

O: 0.01%, Si: 0.12%, Ca: 0.09%, Pd: 99.78%.

The silicon signal is probably due to the silicon substrate and the oxygen to contamination, but the calcium peak cannot be explained by the substrate or contamination.

5. Fission Products

All the new elements that have been produced during these experiments are all lighter than palladium. Therefore, if these elements were created in a nuclear process, the reactions would necessarily be fission reactions induced by hydrogen absorption and laser activation. This mechanism is similar in concept to the fission reactions of ^{235}U when a neutron is absorbed. The elements detected are:

Nitrogen (7), Oxygen (8), Sodium (11), Silicon (14), Phosphorous (15), Sulfur (16), Calcium (20), Manganese (25), Iron (26), Aluminum (27), Nickel (28), Zinc (30), Molybdenum (42), In addition to these elements Mastromatteo [4] observed Titanium (22), maybe due to the intermediate titanium film, and Potassium (19). Same of these elements and some abnormal isotopic ratios were observed by Yamada, et al., while permeating Pd with H_2. [6]

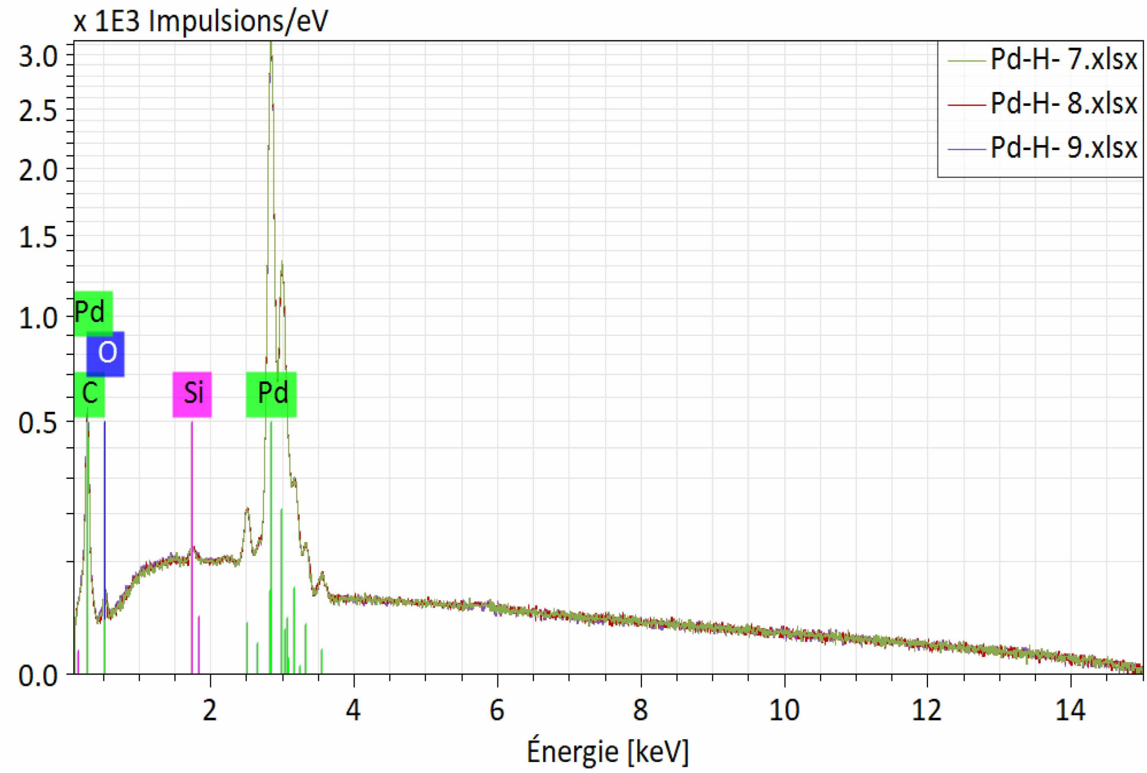

Figure 5. EDX spectra of the three points analyzed in the white area.

A fission parameter, Z^2/A, defines nucleus stability by ratioing the nucleus surface area to its volume and the competition between the attractive strong and repulsive electromagnetic forces [7] where Z is the nuclear charge and A the number of nuclei in the nucleus.

Although calculated for the spontaneous fission of actinides, $Z>88$, related calculations [7] show fission is possible when:

$$Z^2/A > 17, \text{ which for } {}^{46}\mathrm{Pd}_{105} = 20.2$$

Although the fission parameter suggests fission is possible, *it is not probable* without "assistance". Neither does the fission parameter take into account nuclear shell calculations nor nuclear spin, J and parity. Five of the Pd stable isotopes are spherically symmetric with $J = 0+$. The sixth stable isotope's nucleus, ${}^{46}\mathrm{Pd}_{105}$, is oblique with $J = 5/2+$.

6. Neutrons and Alpha Particles Detection

When a palladium atom breaks-up and lighter elements are produced either extra neutrons are emitted or neutron-rich, short half-life daughters are produced [8], [9]. Stable elements lighter than Pd have a neutron/proton ratio lower

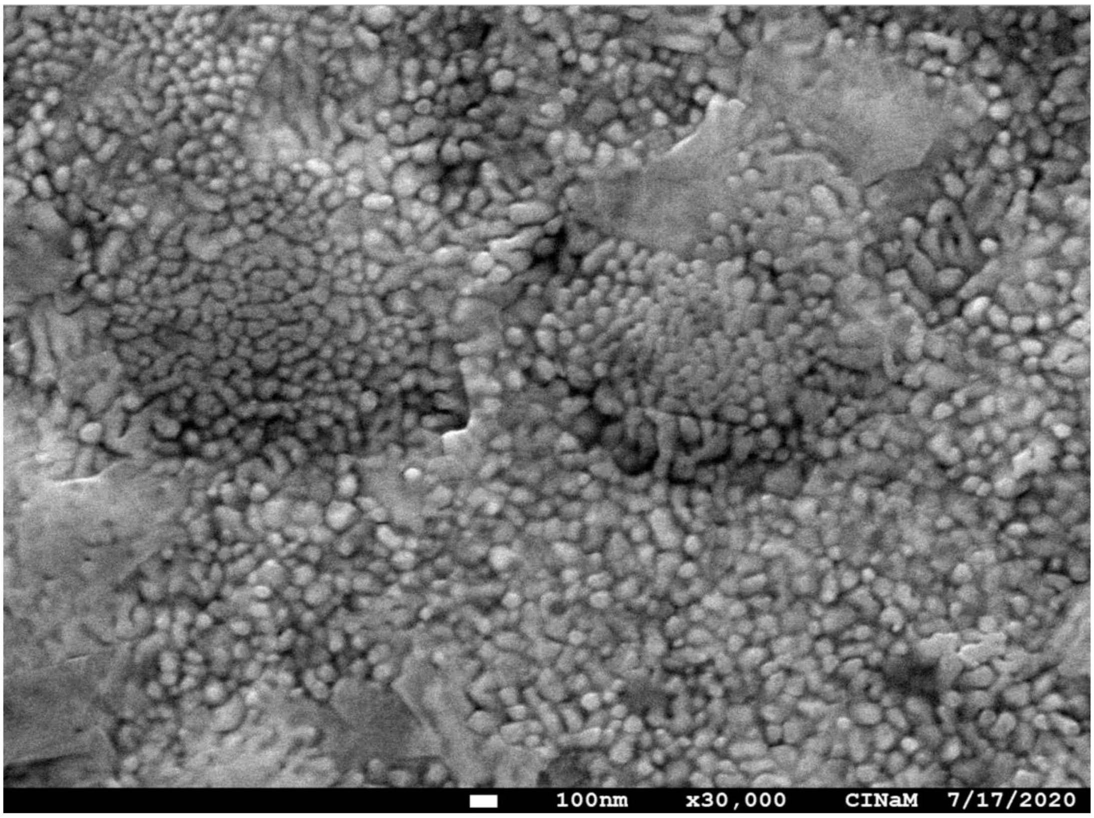

Figure 6. SEM image of the palladium sample after exposure to deuterium for 3 months.

than palladium. Alternatively, the neutron surplus will appear as fast neutrons. Therefore, a second experiment was conducted with the same sample in hydrogen, with the CR-39 detector placed below and above the sample with a control 30 cm away from the sample. Each of the CR-39 detectors has a laser inscribed number on one side. The orientation of the detectors numbered or obverse sides relative to the sample weren't recorded.

Upon completion of the experiment, the CR-39 detectors were etched and underwent both microscopic examination and analysis using a TASL automated scanner. Two scans of the CR-39 have been made on both sides of the three CR-39. One side has laser cut numbers and the reverse, or obverse side, does not.

6.1. CR-39

Three solid-state nuclear track detectors were examined in detail. A ^{241}Am 5.2 MeV alpha source was used for calibration in a corner of the numbered side. Calibration serves to verify etching proceeded normally and as a reference for alpha track major and minor axes distributions. The alpha track diameters averaged 7 – 9 microns which is smaller than the expected 10 – 12 microns indicating the CR-39 was slightly under etched. However, the tracks were usable. The CR-39 was initially manually scanned with a microscope, then scanned with a TASL [10] scanner in 2021 and

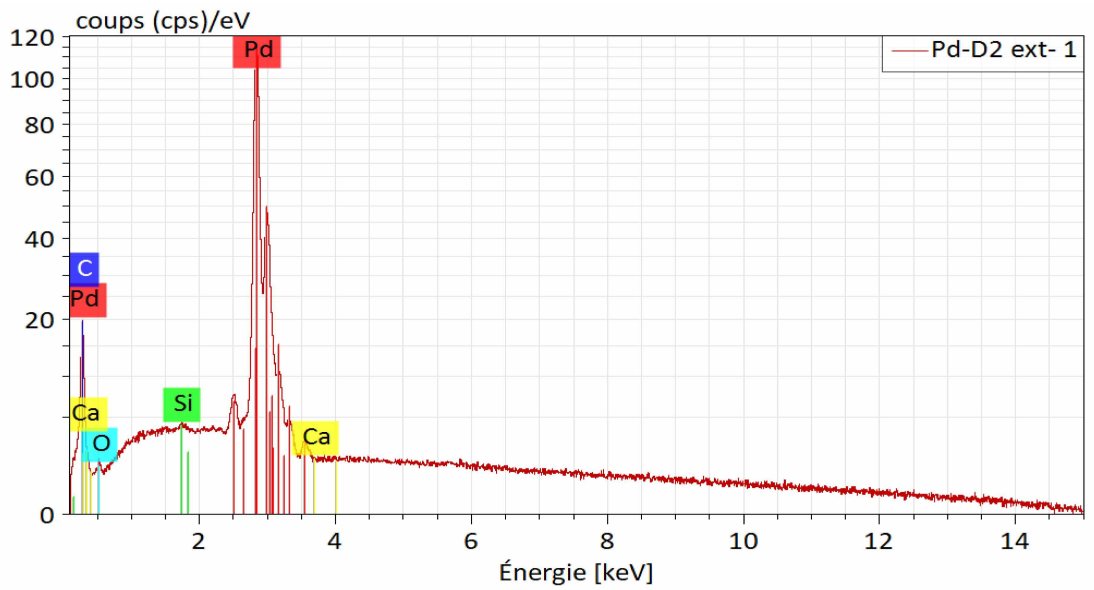

Figure 7. EDX spectra of the three points analyzed in the white area.

Table 1. Comparison of CR-39 Detectors.

Outside control (scanned once)	**Tracks**	**#5521203**	**Tracks/mm^2**	**vs control area**
Scan 1: Numbered	189		3.8	
Scan 1: Obverse	145		2.9	
Under sample (scanned twice)		**#5521403**		
Scan 1: Numbered	1596		39.9	10.5 x
Scan 1: Obverse	6980		175.0	60.3 x
Scan 2: Numbered	1949		39.0	10.3 x
Scan 2: Obverse	2206		44.1	15.2 x
Above sample (scanned once)		**#8203219**		
Scan 1: Numbered	Not scanned			
Scan 1: Obverse	1538		30.8	10.6 x

2023. The detector outside of the experimental apparatus was treated as a control and had few tracks. Each of the CR-39 detectors has a laser inscribed number on one side, for example detector #8203219 that was placed above the sample.

6.1.1. *Setup*

A CR-39 detector was placed under the sample at 45° from the laser beam, and a CR-39 was placed above the sample at 45° from the sample as shown in Figure 8.

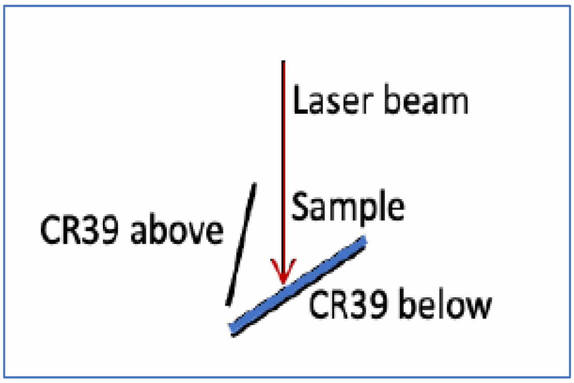

Figure 8. Schematic of the position of the CR-39 detectors below and above the sample.

6.1.2. *Alpha Measurements*

Figure 9 shows a comparison between the *Under Sample* and the *Outside, Control Sample*, showing the alpha particle major axis has a peak count at 6.4 microns. Unfortunately, we had not scanned the alpha calibration region of the CR-39 detector placed *above the sample*, #8203219. However, we are confident that as these detectors were etched at the same time in separate test tubes, the alpha distribution would be nearly identical across all the CR-39. Note the y axis, count, scaling differences in Figure 9.

Alpha diameter distribution regions are noted on other plots. However, these are not from the calibration and likely are either from neutron recoils or ever present alphas in the background from uranium decay daughters. As Table 1 indicates, there are an order of magnitude more tracks on the CR-39 observing the experiment than on the control.

6.1.3. *Comparison of Obverse sides*

Figure 11 compares the alpha region with the track distributions for all three detectors on the obverse (non-numbered) side. It is noteworthy the order of magnitude larger number of tracks on the above and under sample detectors. There is an inverse relationship between the track size energy/charge as seen in Figure 10 with fast protons. [11]

It is most likely the tracks assigned as fast neutron recoils are from fast neutrons hitting hydrogen in the CR-39: $(C_{12}H_{18}O_7)_n$ or the polyethylene (PE) $(C_2H_4)_n$ cover on one side. Although PE blocks protons < 3 MeV and alphas < 8 MeV, it also acts as a neutron "radiator" by providing PE hydrogen and carbon nuclei for recoil.

It isn't unusual that there would be some fast neutrons impinging on the control, although there are over 20x more tracks of this diameter. It is striking that there are two distinct, adjacent peaks found on the above and under sample's CR-39. Since neutron recoils can produce tracks of varying radii, even for the same energy, this would suggest very fast protons made the tracks. However, the next figure comparing the obverse and numbered sides argues against this. It takes over a 10 MeV proton to traverse a 1 mm thick CR-39 yet the linear energy transfer (LET) loss from a fast proton would change the track distribution on the two surfaces of the CR-39.

Similarly, assuming activation of the Pd occurs on the side facing the laser, only neutrons could traverse the Pd to reach the CR-39 beneath the sample. The alpha region in Figure 11 refers to the track size and is indicated consistent with the track diameter observed from the ^{241}Am calibrations on each detector as in Figure 9. However, tracks in this

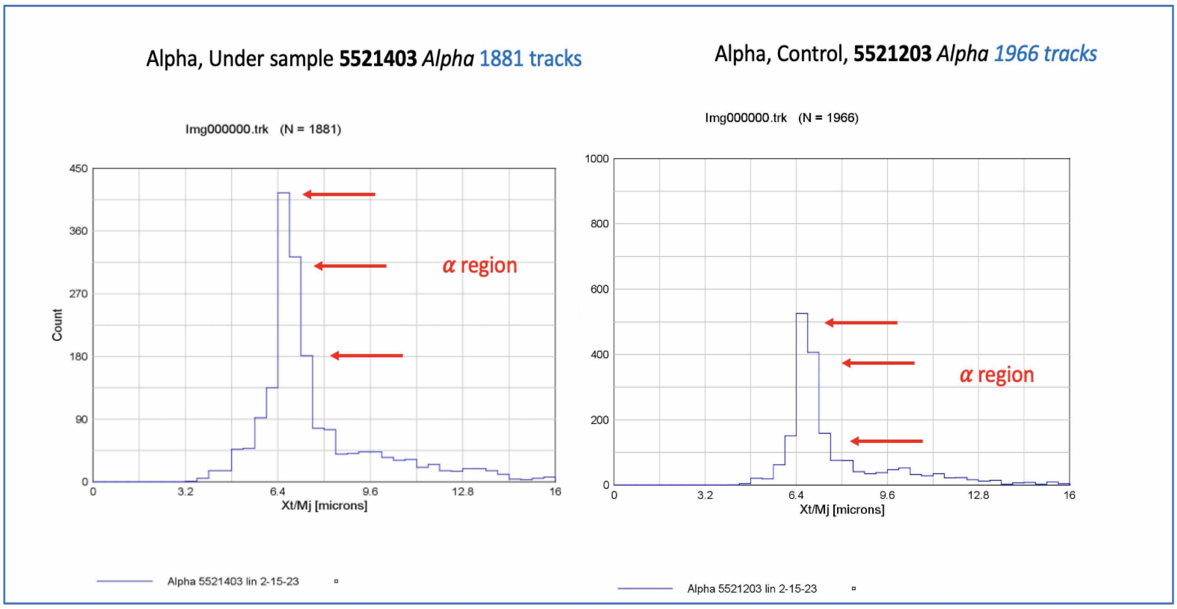

Figure 9. Comparison between alphas detected by the under sample and the control.

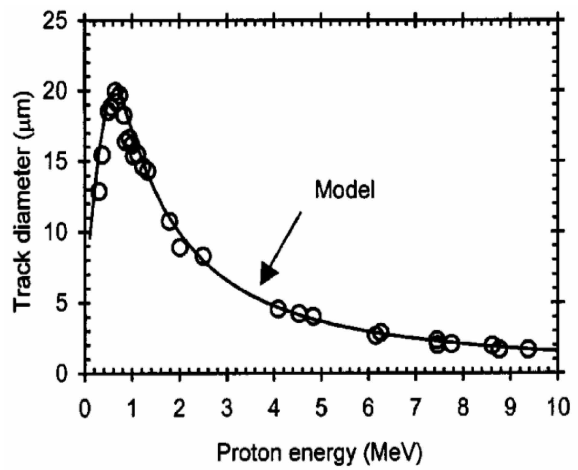

Figure 10. Proton track diameter vs energy [11].

region aren't from the calibration and may be from ever present background alpha tracks or oblique neutron recoils. The latter may originate from either cosmogenic background neutrons or from the experiment. The orders of magnitude increase in smaller tracks on the experimental CR-39 as compared to the control indicate these aren't background.

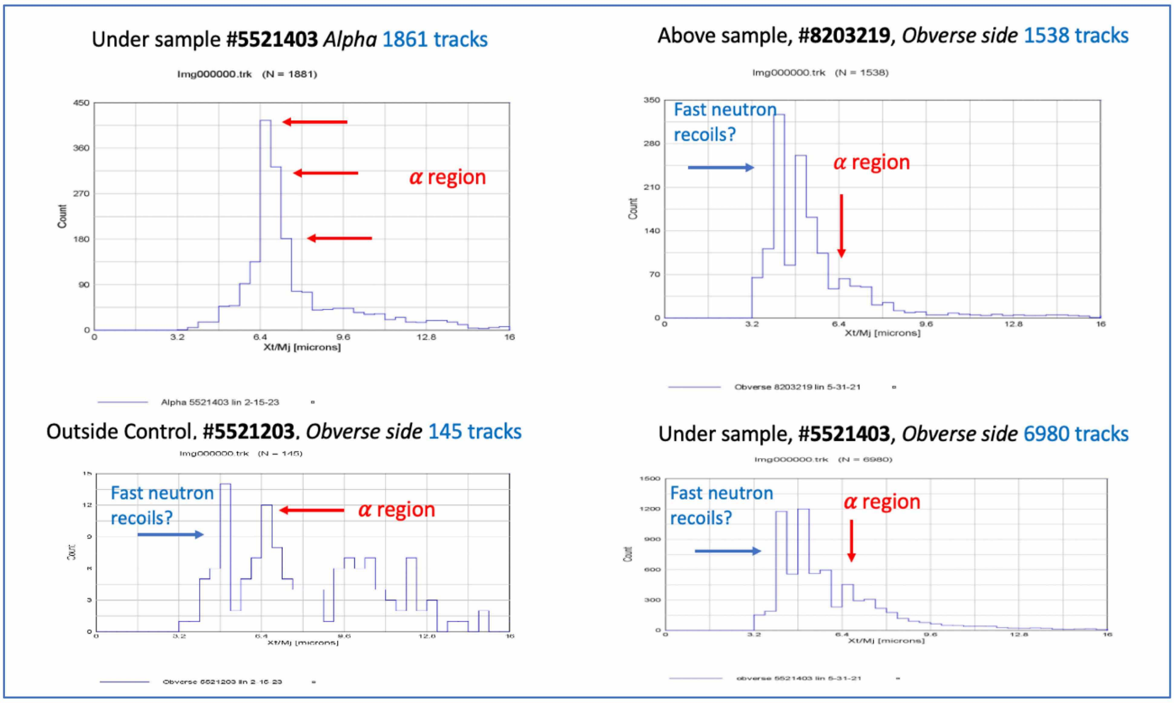

Figure 11. Comparison between the under sample and the obverse side of the three detectors: above, outside and under.

6.1.4. *Comparison of obverse and numbered sides*

Detector 5521403 from under the sample was scanned twice as shown in Figure 11. The earlier comparison with the obverse side of the detector above the sample shows a similar dual peak in the count distribution. There is an inconsistency between the first and second scans of the under sample detector 5521403 on the obverse side with 6980 tracks identified the first time but only 2206 tracks the second. This is due to a different area of the detector being scanned each time. It is worth noting that the numbered side of the same CR39 detector had comparable numbers of tracks, 1596 and 1949 from the two scans conducted.

There are strong indications of fast neutron or fast proton interactions given a pair of peaks indicating more kinetic energy than the alpha controls. One of these peaks appears on the control, but with 20x fewer counts. It's worth noting that Pd fission neutrons will not have 2.45 MeV energy unlike DD fusion neutrons. Rather, fission neutrons can be expected to have energies on the order several MeV with their kinetic energy inversely proportional to the Pd fission fragment mass and their energy.

The consistency of two, small diameter double peaks on both the obverse and numbered sides of the CR-39, regardless of its orientation relative to the surface of the Pd sample, is significant. It may indicate two different, but nearly equal, fast energy neutron distributions. These distributions may reflect the number of fragments, and their masses, from Pd fission. The energy of the second peak, as seen in the control from cosmogenic neutrons, suggests an energy similar to that found at the 2.5 MeV cosmogenic peak seen in Figure 12 whereas the smaller peak from a smaller diameter track has a higher energy.

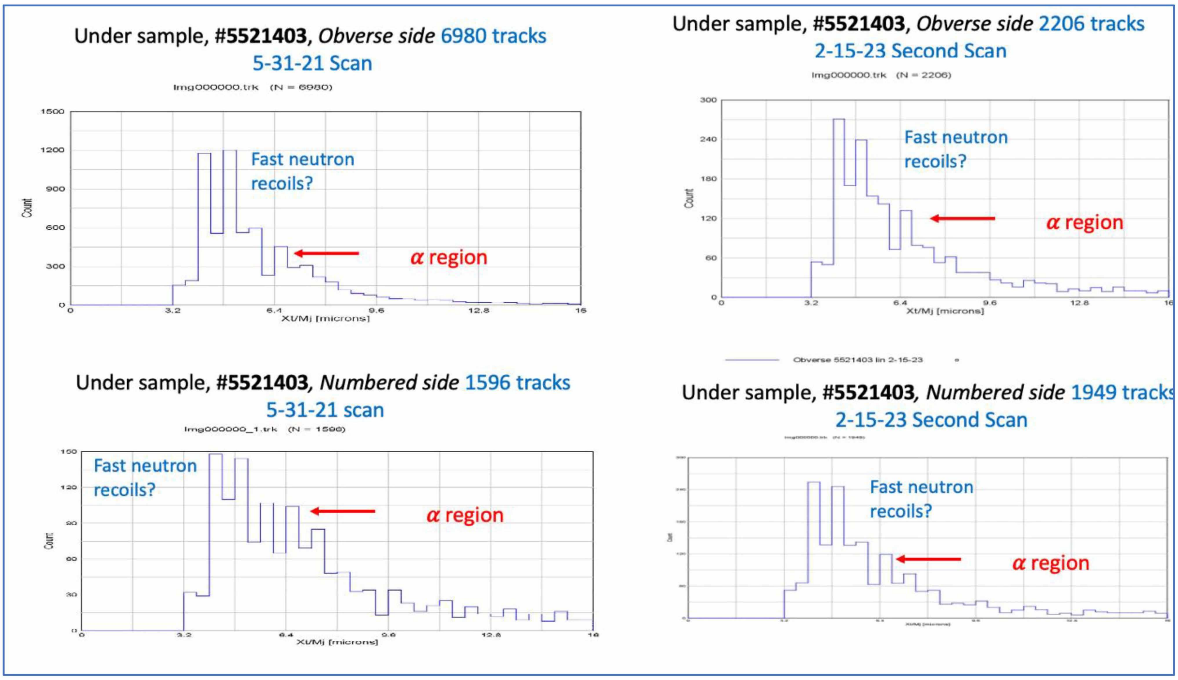

Figure 12. Comparison between scans made in years 2021 and in 2023.

6.1.5. *CR-39 Area Scanned*

Figure 13 shows the area scanned as a montage of microphotographs on the left, the coordinate distribution of identified tracks in the middle and their major axis (Xt) distribution for detector #5521403, Under Sample on the obverse side. As noted earlier, this is from the 2-15-23 scan. The nearly 3 fold difference in counts is due to different areas of the detector being scanned.

6.1.6. *Cosmogenic Neutrons*

Cosmogenic spallation neutrons complicate detecting DD fusion neutrons as noted by Goldhagen [12] in Figure 14. There are three main peaks: thermal (.025 eV), 2.5 MeV with some adjacent peaks, and another at 100 MeV. Note that the 2.5 MeV peak overlaps the DD fusion 2.45 MeV neutron energy. This spectrum was taken in Livermore, CA prior to October, 2015. These neutrons provide a background source of the tracks on both sides of the control detector and the experimental detectors.

7. Conclusion

We have shown in this experiment that hydrogen absorbed in a thin film of palladium under the excitation of a 5 mW laser pointer (650 nm of wavelength) apparently induces new elements not present in the initial palladium film. These new elements are all lighter than palladium and are therefore are the *result of a fission process*. These results confirm

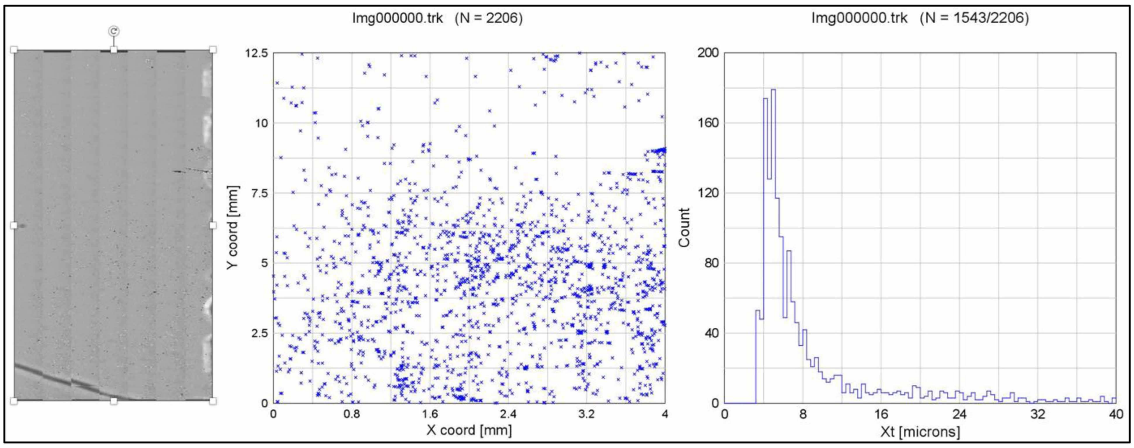

Figure 13. #5521403 Under Sample Area Scanned and Diameter (Xt) plotted.

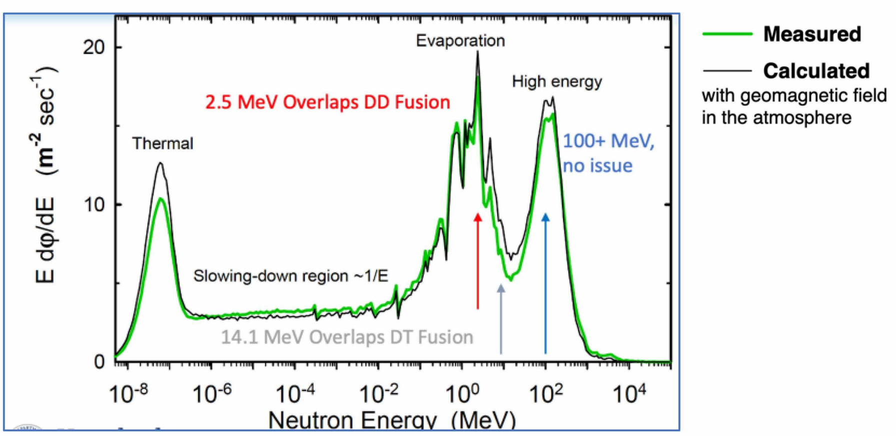

Figure 14. Cosmogenic Spallation Neutron Spectra [12].

that of Mastromatteo [5]. One may think that these elements are local impurities, but we have observed large quantities of nitrogen, and this cannot be a contamination when the sample is brought to air, since it is very difficult to break the nitrogen molecular bonds. Furthermore, PdN_2 is thermodynamically unstable [13]. Another experiment had CR-39 detectors to measure the production of neutrons, protons and alpha particles. We likely detected two populations of fast neutrons at over 10x background. These results are very important for the development of a Low Energy Nuclear Reaction (LENR) theory.

Acknowledgment

We wish to thank Ubaldo Mastromatteo for giving us the two palladium samples and Victoria Leist for doing the CR-39 analysis. CR-39 analysis was supported by the Anthropocene Institute under the Trackers STEM Program^{TM}.

References

[1] Y. Arata and Zhang, Y.-C., Anomalous difference between reaction energies generated within D_2O-cell and H_2O-cell, *Jpn. J. Appl. Phys.* Pt.2 **37** (11A), L1274, (1998).

[2] M.C.H. McKubre, Tanzella, F. L., Tripodi, P., and Hagelstein, P. L., "The emergence of a coherent explanation for anomalies observed in D/Pd and H/Pd system: evidence for ^{4}He and ^{3}He production", *8th International Conference on Cold Fusion*, Scaramuzzi, F. Ed. *Italian Physical Society*, (Bologna, Italy, Lerici (La Spezia)), Italy, (2000), p. 3.

[3] J.P. Biberian, "Anomalous Isotopic Distribution of Silver in a Palladium Cathode", *J. Condensed Matter Nucl. Sci.* **29** (2019) pp. 211–218.

[4] T.Mizuno, "Transmutation Reactions in Condensed Matter", *Low Energy Nuclear Reactions Sourcebook*, *Vol. 1*, Marwan, J. and Krivit, S. B., (Eds,), American Chemical Society, Washington D.C, Oxford University Press, Oxford, (2008).

[5] U. Mastromatteo, "LENR Anomalies in Pd–H_2 Systems Submitted to Laser Stimulation", *J. Condensed Matter Nucl. Sci.* **19** (2016) pp. 173–182.

[6] H. Yamada, S. Narita, H. Onodera, H. Suzuki, Ntanaka, T. Nyui and T. Nyui and T. Ushirozawa, "Analysis By Time-Of-Flight Secondary Ion Mass Spectroscopy or Nuclear Products In Hydrogen Penetration Through Palladium", *ICCF-10*, (Cambridge, MA) (2003).

[7] K.N. Mukhin, *Experimental Nuclear Physics, Vol I, Physics of Atomic Nucleus,* MIR Publishers (Moscow, Russia) (1987) pp. 461–464.

[8] T. L. Benyo, W. Jennings, L. Forsley, B. Steinetz, G. Fralick, R. Hendricks, "A Theory for Transmutations Resulting from Deuterium Gas Cycling of PdAgAlloy", *ICCF-24: Solid State Energy Summit* (Mountain View, CA), (July 28, 2022)

[9] T. L. Benyo, P.A. Mosier-Boss, L. Forsley, W. Jennings, G. Fralick, R. Hendricks, "LENR Products: Lattice Confinement Fusion (LCF), Fission, or Both?", Submitted to *ICCF-25*.

[10] https://www.tasl.co.uk

[11] F. H. Seguin, *et al.*, "Spectrometry of charged particles from inertial-confinement-fusion plasmas**",** *Review of Scientific Instruments,* **74**(2) (February 2003) p. 979 Figure 6.

[12] P. Goldhagen, "Use of Cosmic-Ray Neutron Data in Nuclear Threat Detection and Other Applications", *Neutron Monitor Community Workshop*, (Honolulu, Hawaii) (October, 2015) pp. 11.

[13] W Chen *et al*, "Stability, elastic and electronic properties of palladium nitride", *J. Phys.: Condens. Matter* **22** (2010) 015404.